Design of Compact RF Filters with Narrow Band-Pass and Wide Stop-Band by Open-Stub & T-shaped Microstrip Resonators and Defected Ground Structure (DGS)

Shervin Amiri [1], Nafiseh Khajavi [2], Mahboubeh Khajavi [3]

[1]Scientific Member of E.E Department of IROST, Tehran, Iran, amiri@irost.ir

[2,3]Faculty of E.E Department of Dezful Branch of Islamic Azad University, Dezful, Iran, N_khajavi89@yahoo.com , Zefins2011@yahoo.com

Abstract- This paper presents the design of a narrow band-pass filter with wide stopband for WLAN and WiMAX applications. First, open-stub and T-shaped resonators were used to design a filter (F1) with the center frequency of 2.4 GHz. In order to verify the architectures of the proposed resonators, their frequency responses were compared to the response of an LC model. Next, DGS was utilized to achieve a wide stopband within the frequency response of F1. The design of other narrow-band filters (F2 and F3) with their center frequencies of 3.7 GHz and 5.1 GHz respectively is derived only by modifying the dimensions of the resonators in the structure of F1.Advantages of these filters include simplicity, architectural symmetry, tuning for applications at other frequencies and proper bandwidth. These filters have optimal return loss and insertion loss.

Keywords- Compact microstrip filters, Narrow Band-pass, Wide Stop Band, Defected Ground Structure (DGS)

.

I. INTRODUCTION

High-quality compact bandpass filters are among the common elements in wireless communication systems. Wide-stopband filters are used in nonlinear elements such as power amplifiers or mixers for rejecting noise or unwanted interference in the stopband. Bandpass filters with wide stopbands may be designed for different frequencies. The frequencies of 2.4 GHz and 5.1 GHz are consistent with the IEEE 802.11 standards for WLAN systems while the frequency 3.7 GHz is among the operating frequencies for WiMAX technology. There are different techniques for designing narrow-band filters with wide stopbands. For example, ring resonators have been used to eliminate the second harmonic in a bandpass filter with the center frequency 2.6 GHz. This narrow-band filter, however, does not have an acceptable insertion loss [1]. A narrow bandpass filter has been designed by eliminating the harmonic $11f_0$ using various types of quarter-wavelength SIRs[2]. The insertion loss at the center frequency of this filter (2.4 GHz) is at the non-optimal level of 2.6 dB. DGS has been used to improve the filter parameters, including its bandwidth. Dumbbell-shaped DGS (DS-DGS) was implemented at the ground structure [3]. A bandpass filter with the center frequency 2.4 GHz has been designed by coupling two open-loop DGS slot resonators with microstrip resonators [4]. DGS technique has also been implemented on bandpass filter structures to examine how this technique impacts the results [5]. A compact microstrip single-band bandpass filter with controllable bandwidth has been designed by coupling two DGS resonators. The center frequency of this filter does not match the frequency of WLAN applications. In addition, the insertion loss of this filter is above 1 dB [6]. In this paper, a single-band bandpass filter with a wide pass band was designed by cascading a low-pass and a bandpass filter [7]. An LC model has been developed for microstrip lines [7-11].

This paper presents narrow-band bandpass filters with wide stopbands for WLAN and WiMAX applications. Open-stub and T-shaped resonators were used to design the architecture of the filters. The frequency responses of these structures were compared to the frequency response of the LC model in order to examine the architecture of the proposed resonators. For the first filter (F1) with the center frequency 2.4 GHz, DGS was applied to improve the width of the stopband. Next, it has been shown that due the simplicity and symmetry in the architecture of this filter, two other filters with the center frequencies 3.7 GHz (for F2) and 5.1 GHz (for F3) can be constructed only by modifying the dimensions of the resonators. All simulations in this paper were implemented using Momentum simulator in ADS software.

II. DESIGNING FILTER F_1

Using open-stub resonators placed in parallel to each other (the resonators are connected through a middle stub), the basic resonator architecture shown in Fig. 1(a) was obtained. As seen in the frequency response of the basic resonator (Fig. 1(b)), this architecture has a resonance frequency of 2 GHz with insertion loss of 0.22 dB and a return loss of 32.88 dB. The presence of a neutral harmonic at 5.46 GHz limits the stopband. In addition, the center frequency of this architecture does not match the WLAN frequency. The dimensions of the basic resonator are: L1 = 5.3 mm, W1 = 0.1 mm, L2 = 6.4 mm, W2= 0.1 mm, L3 = 20.06 mm, W3= 0.1 mm and G1= 4.788 mm.

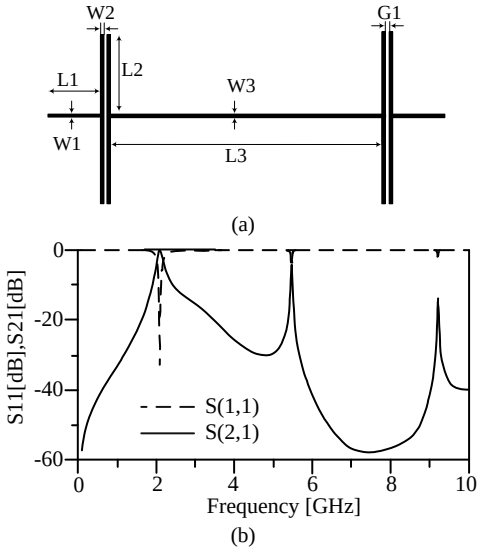

Fig.1 (a) Basic structure of the proposed resonator.(b) Frequency response of basic structure of the proposed resonator.

ISBN: 978-1-61804-215-6

An LC model is presented to further examine the basic resonator. The effective dielectric constant ε_{re} and characteristic impedance Z_C are used to identify the characteristics of microstrip lines [12]. For substrate R04003 with the thickness H=20Mil and a microstrip line with the width W (The width of microstrip lines are presented in Fig. 2), ε_{re} can be obtained from (1).

$$\begin{cases} \varepsilon_{reff} = \dfrac{\varepsilon_r+1}{2} + \left\{\left(1+12\dfrac{H}{W}\right)^{-0.5} + 0.04\left(1-\dfrac{W}{H}\right)^2\right\} \dfrac{W}{H} \le 1 \\ \varepsilon_{reff} = \dfrac{\varepsilon_r+1}{2} + \dfrac{\varepsilon_r-1}{2}\left(1+12\dfrac{H}{W}\right)^{-0.5} \dfrac{W}{H} \le 1 \end{cases} \quad (1)$$

Equation (2) is used to calculate C_a. ε_r is the permittivity of dielectric substrate. C_a is capacitance per unit length for an air substrate.

$$\begin{cases} C_a = \dfrac{2\pi\varepsilon_0}{ln\left(\frac{8H}{W}+\frac{W}{4H}\right)} \dfrac{W}{H} \le 1 \\ C_a = \varepsilon_0\left(\dfrac{W}{H}+1.393+0.667ln\left(\dfrac{W}{H}+1.444\right)\right)\dfrac{W}{H} \le 1 \end{cases} \quad (2)$$

L and C are derived from (3). For this purpose, one should first calculate phase velocity V_P and characteristic impedance Z_C.

$$Z_c = \frac{120\pi}{\frac{C_a}{\varepsilon_0}\sqrt[2]{\varepsilon_{re}}} \quad , \quad V_p = \frac{(3.0*10^8)\frac{m}{s}}{\sqrt[2]{\varepsilon_{re}}}$$

and

$$\begin{cases} L = \dfrac{Z_C l}{V_P} \\ C = \dfrac{l}{Z_C V_P} \end{cases} \quad (3)$$

In this model, Lt1 represents the lines which connect the ports to the basic resonator while Lt2 shows the line which connects open-stub resonators together. The gap between the open-stub resonators is denoted by Cg1. The grounded capacitor Cop and the inductor Lop were used to model the open-stub resonators. The LC model is shown in Fig. 2(a). Comparison of the frequency response of the LC circuit with the simulation results indicates a proper match between the center frequencies of both frequency responses shown in Fig. 2(b). The values of inductance and capacitance for the LC model are: Lt1= 3 nH, Lt2= 8.3 nH, Lop= 0.95 pF, Cop= 0.5 pF and Cg1= 0.37 pF.

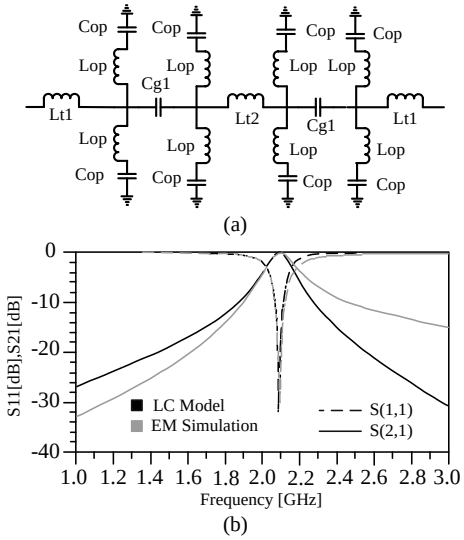

Fig.2 (a) The LC model of the basic structure, (b) Frequency response of the LC model and EM simulation of the basic structure

In the next step, T-shaped resonators were used to improve the stopband and to obtain a center frequency which is consistent with IEEE 802.11a (Fig. 3(a)). The arrangement of the T-shaped resonators has created a deep zero at 5.4 GHz. The dimensions of the T-shaped resonators are: W4=0.247 mm, L4=10.266 mm, W5=1.08 mm, L5=5.74 mm, W6=0.70 mm, L6=1.98 mm and G1=0.24 mm.

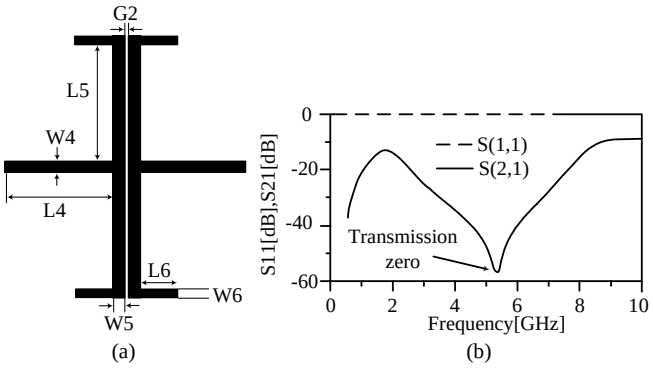

Fig.3 (a) T-shape structure resonators, (b) Frequency response of T-shape structure resonators.

Again, an LC model was used to examine these T-shaped resonators. In this model, the microstrip lines are modeled based on their corresponding indices using inductors and capacitors. Cg2 represents the gap between the T-shaped resonators. The open-ended sections are grounded through a capacitor and the transmission lines are modeled by inductors. The model is shown in Fig. 4(a). The values of the capacitance and inductance are: L4= 0.85 nH, L5= 1.45 nH, L6= 0.5 nH, C6= 0.5 pF and Cg2= 0.1 pF.

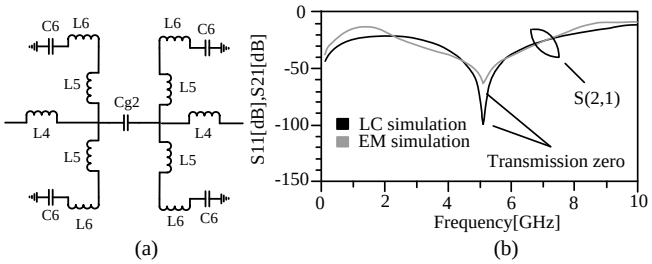

Fig.4 (a) The LC model of the T-shape structure resonators, (b) Frequency response of the LC model and EM simulation of the T-shape structure resonators

A comparison of the frequency response of the LC model for the T-shaped resonators and the associated EM simulation indicates a good match between the two simulations as seen in Fig. 4(b). The presence of a deep zero at 5.4 GHz along with a frequency response with a pole at the same frequency cancels the effect of the zero and the pole at this frequency, thereby widening the stopband. This can be seen in Fig. 5. These results in center frequency of 2.69 GHz are insertion loss of 4.36 dB, and return loss of 2.5 dB, which show a considerable drop in losses compared to the frequency response obtained for open-stub resonators.

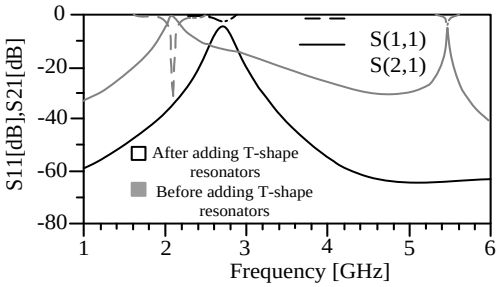

Fig.5 Comparison the frequency response of basic structure before and after adding the T-shaped resonators

In fact, the final architecture of filter F1 was obtained by putting together the open-stub resonators and the T-shaped resonators. The architecture is shown in Fig. 6(a). Desirable center frequency, insertion loss, return loss, and

bandwidth were achieved by optimizing the dimensions of different parts of the open-stub and T-shaped resonators. The dimensions of the filter structure F_1 are:
W1=0.1mm, L1=3.06mm, W2=0.34mm, L2=6.50mm, W3=0.1mm, L3=1.35mm, W4=0.24mm, L4=10.26mm, W5=1.08mm, L5=5.74mm, W6=0.70mm, L6=1.98mm, G2=0.24mm and G1=0.18mm.
As seen in the frequency response of F1 (Fig. 6(b)), return loss and insertion loss for this filter are 32.8 dB and 0.5 dB, respectively. The bandwidth of F1 is 112 MHz.

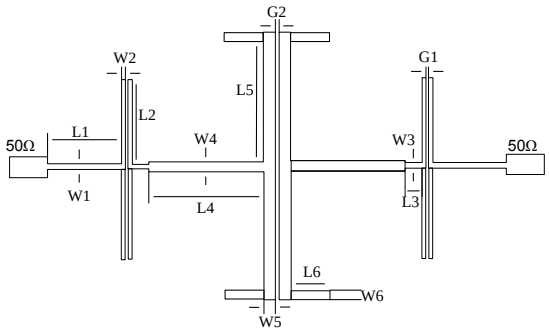

(a)

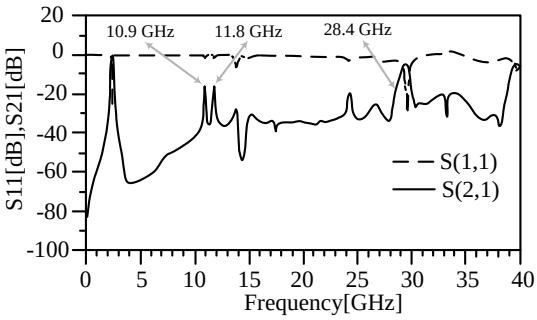

(b)

Fig.6 (a) Structure of the filter F_1 (b) Frequency response of filter F_1

Fig. 7 shows a schematic of constructed filter and a comparison of its measured frequency response to that of the simulation model. As seen in Fig. 7, the two responses are in close agreement.

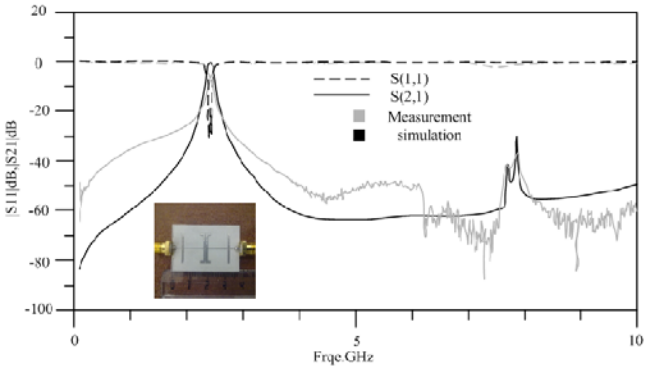

Fig.7 Comparison of the results EM-simulation and measurement for filter F1

III. Adding DGS to Structure of the Filter F_1

The presence of some harmonics at 10.9 GHz, 11.8 GHz, and 28.4 GHz in the frequency response of F1 (Fig. 6(b)) has limited the stop-band of the filter. DGS was used to eliminate the neutral harmonics in the stopband and to widen this band. DGS technique was employed to create the dumbbell-shaped structure shown in Figure 8.

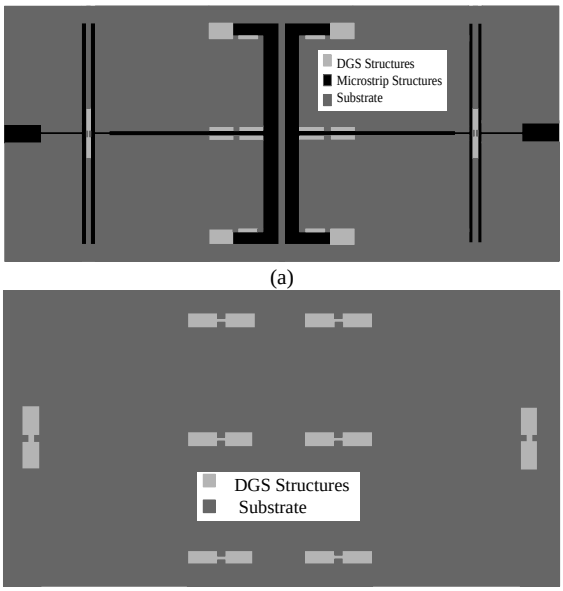

(a)

(b)

Fig.8 (a) The architecture seen from above (b) The substrate and dumbbell-shaped DGS structure seen from below

Fig. 9 compares the frequency responses of filter F1 before and after applying DGS. Applying DGS shifts all the neutral harmonics in the stopband, up to the frequency 39 GHz, into the levels below -20 dB, thereby widening the stopband by 16.25 F_0.

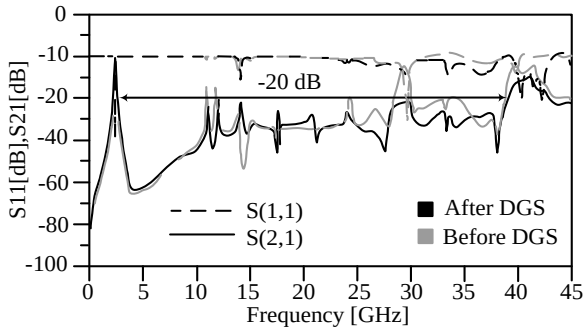

Fig. 9 compares the frequency responses of filter F1 before and after applying DGS

According to the comparison presented in Table I, DGS improves not only the stopband, but also return loss and insertion loss.

Table.1 Comparison of the results for filter F1 before and after applying DGS

Filter F_1	Center frequency	Limit of the stop band	Band width	Return loss	Insertion loss
Before DGS	2.42GHz	$12f_0$	0.121GHz	33.35dB	0.521 dB
After DGS	2.42GHz	$16.25F_0$	0.121GHz	38.3 dB	0.426 dB

IV. Designing Filters with Center Frequency of 3.7GHz and 5.1GHz

One objective in designing microstrip filters is to design small size architectures with high capabilities which are regarded as advantages of this type of architecture. These small and highly capable architectures can be designed by combining open-stub resonators with T-shaped resonators. Therefore, F2 with the center frequency 3.7 GHz and F3 with the center frequency 5.1 GHz were obtained simply by changing the dimensions of filter

F1. Filters F1 and F3 can be used in WLAN applications while filter F2 is suitable for WiMAX systems.

V. DESIGNING FILTER F_2

The architecture of this filter is the same as the architecture of filter F1 and the optimized dimensions are: W1=0.1 mm, L1=5.3 mm, W2=0.16 mm, L2=6.4 mm, W3=0.1 mm, L3=0.5 mm, W4=0.8 mm, L4=8.88 mm, W5=0.8 mm, L5=5.4 mm, W6=0.4 mm, L6=1.6 mm, G1=0.2 mm and G2=0.15 mm.

The frequency response of this filter is shown in Fig. 10. As seen in this figure, filter F2 has its center frequency at 3.7 GHz, a bandwidth of 214 MHz, an insertion loss of 0.42 dB, and a return loss of 41.578 dB. Since magnitude of S21 is below -20 dB, for frequencies up to 11.79 GHz, the first, second, and third harmonics are eliminated in filter F2.

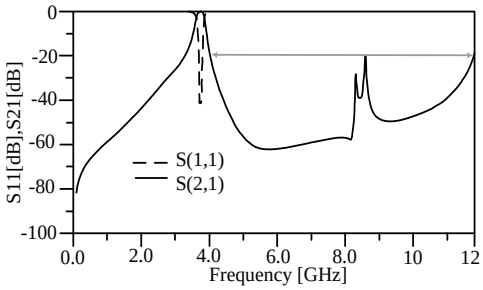

Fig.10 frequency response of the filter F_2

VI. DESIGNING FILTER F_3

The architecture of this filter is the same as the architecture of filter F1 and the optimized dimensions are: W1=0.1 mm, L1=4.69 mm, W2=0.12 mm, L2=4.48 mm, W3=0.1 mm, L3=0.76 mm, W4=0.56 mm, L4=6.16 mm, W5=0.616 mm, L5=3.66 mm, W6=0.397 mm, L6=1.12 mm, G1=0.14 mm and G2=0.105 mm.

The frequency response of this filter is shown in Fig. 11. As seen in this figure, filter F3 has its center frequency at 5.1 GHz, a bandwidth of 423 MHz, an insertion loss of 0.318 dB, and a return loss of 53.23 dB. Since magnitude of S21 is below -20 dB, for frequencies up to 16.27 GHz, the first and second harmonics are eliminated in filter F3.

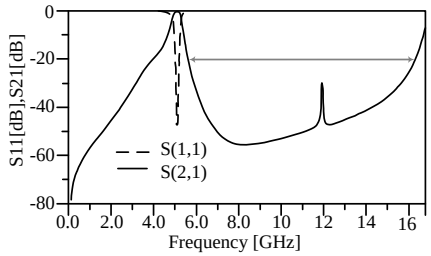

Fig.11 frequency response of the filter F_3

Comparison of the dimensions of these three filters demonstrates that for higher center frequencies, the sizes of the filter will be smaller as expected; frequency has an inverse relationship to size. Table II compares the results obtained for the filters designed in this paper. Frequency responses of the three filters are shown in Fig. 12.

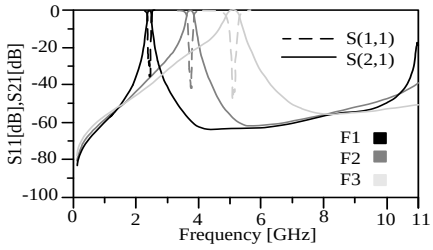

Fig.12 Frequency responses of the three proposed filters

Table.2 Final results for optimized architectures of the proposed microstrip single-band bandpass filters

Filter name	Center frequency	Insertion Loss	Return loss	Band width	Limit of the stop band	Size of the filter
F1	2.42GHz	0.521 dB	33.35 dB	0.121 GHz	$12f_0$	37.182*13.45 mm^2
F2	3.7GHz	0.42 dB	41.57 dB	0.214 GHz	$3f_0$	36.46*12.91 mm^2
F3	5.1GHz	0.318 dB	53.23 dB	0.423 GHz	$2f_0$	29.81*9 mm^2

VII. CONCLUSION

This paper presents narrow-band bandpass filters with wide stopband for WLAN and WiMAX applications. First, using parallel open-stub resonators, the frequency response of the basic resonator was obtained with the resonance frequency 2 GHz and a pole at 5.4 GHz. T-shaped resonators were placed next to open-stub resonators, to cancel this pole, widen the stopband, and construct the final architecture for F1. The T-shaped resonators create a deep zero at the same frequency, thereby cancelling the effect of this pole.

To examine the architectures of the proposed resonators, the frequency responses of these architectures were compared with the frequency responses of their corresponding LC model. Then, narrow-band filters with the center frequencies 3.7 GHz and 5.1 GHz (for F2 and F3, respectively) were obtained simply by changing the dimensions of the resonators in the basic structure of F1. Finally, DGS was utilized to achieve a wide stopband in the frequency response of F1. An advantage of these filters is having a good bandwidth. In addition, these filters have optimal return loss and insertion loss. In this paper we obtained: (a) Comparison of frequency responses before and after adding the T-shaped resonators. (b) Comparison of the results for F1 before and after applying DGS. (c) Frequency responses of the three proposed filters. (d) Final results for optimized architectures of the proposed microstrip single-band bandpass filters.

REFERENCES

[1] J. Fraresso and C.E. Saavedra, "Narrowband bandpass filter exhibiting harmonic suppression," Electronics letters, Vol. 39, No. 16, 1189-1190, 2003.

[2] S-C. Lin, P-H. Deng, Y-S Lin, C-H. Wang, and C. H. Chen, "Wide-Stop band Microstrip Bandpass Filters Using Dissimilar Quarter-Wavelength Stepped-Impedance Resonators," IEEE transactions on microwave theory and techniques, Vol. 54, No. 3, 1011-1018, 2006.

[3] A. Kumar, M.V. Kartikeyan, "A design of microstrip bandpass filter with narrow bandwidth using DGS/DMS for WLAN," Communications (NCC), 2013 National Conference on, New Delhi, India, 1-4, 2013.

[4] P. Vagner, M. Kasal, " A Novel Bandpass Filter Using a Combination of Open-Loop Defected Ground Structure and Half-Wavelength Microstrip Resonators," Radioengineering, Vol. 19, No. 3, 392-396, 2010.

[5] M. Kufa, Z. Raida, "Comparison of Planar Fractal Filters on Defected Ground Substrate," Radioengineering, Vol. 21, No. 4, 1019-1024, 2012.

[6] S. U. Rehman, A. F. A. Sheta, and M. A. S. Alkanhal, " Compact Bandpass Filters with Bandwidth Control using Defected Ground Structure (DGS)," ACES Journal, Vol. 26, No. 7, 624-630, 2011.

[7] M. Shobeyri and M. H. Vadjed Samiei, "Compact ultra-wideband Bandpass Filter With Defected Ground Structure," Progress In Electromagnetics Research Letters, Vol. 4, 25–31, 2008.

[8] T. Yang, M. Tamura, and T. Itoh, "Compact Hybrid Resonator With Series and Shunt Resonances Used in Miniaturized Filters and Balun Filters," IEEE Transactions on microwave theory and techniques, Vol. 58, No. 2, 390-402, 2010.

[9] Z.-C. Hao, and J.-S. Hong, UWB Bandpass Filter Using Cascaded Miniature High-Pass and Low-Pass Filters With Multilayer Liquid Crystal Polymer Technology," IEEE Transactions on microwave theory and techniques, Vol. 58, No. 4, 941- 948, 2010.

[10] F. Wei, C.-J. Gao, B. Liu, H.-W. Zhang and X.-W. Shi, "UWB bandpass filter with two notch-bands based on SCRLH resonator," Electronics letters, Vol. 46 No. 16, 2010.

[11] F. Wei, Q. Y. Wu, X. W. Shi, and L. Chen, "Compact UWB Bandpass Filter With Dual Notched Bands Based on SCRLH Resonator," IEEE microwave and wireless components letters, Vol. 21, No. 1, 28-30, 2011.

[12] J. S. Hong, and M. J. Lancaster, "Microstrip Filters for RF/ Microwave Applications," Book (Hong, et al., 2001), A Wiley-Interscience Publication, John Wily & Sons, Inc, 2001.

1) **Shervin Amiri** is Scientific Member of Electrical Engineering Department of Iranian Research Organization for Science and Technology (IROST) in Tehran, I.R.Iran. He received to associate professor degree at 2013. His research interest fields are Antenna and RF subsystems in microwave and millimeter wave bands. He is supervisor of many MSc and PhD students in these fields.

2) **Nafiseh Khajavi** received the B.Sc. degree in Medical Engineering from Islamic Azad University Dezful branch, Iran, 2007, and the M.Sc. degree in Electrical Engineering from Kermanshah Science and Research Branch Islamic Azad University, Kermanshah, Iran, 2012. She has been with the Department of Engineering Islamic Azad University Dezfull branch. Her research interests include microstrip filter, the analysis and design of high-frequency electronics and microwave passive circuits.